Optical system optimization method for as-built performance based on nodal aberration theory

ZHIYUAN GU,[1,]* [iD] YANG WANG,[2] AND CHANGXIANG YAN[1]

[1] *Changchun Institute of Optics, Fine Mechanics and Physics, Chinese Academy of Science, Changchun, 130033, China*
[2] *School of OptoElectronic Engineering, Changchun University of Science and Technology, Changchun, 130022, China*
zhiyuan.gu@hotmail.com

Abstract: The traditional optical design process isolates the two steps of system performance optimization and tolerance allocation, making it difficult to achieve optimal design of as-built performance. To solve this problem, this paper proposes an analytical method for optimizing the as-built performance of optical systems. The method uses the nodal aberration theory to derive the wavefront aberration estimated value under the given surface decenter and tilt tolerance, and establishes the optical system as-built performance evaluation model. The as-built performance evaluation does not require a large amount of ray tracing, which can be completed only by tracking the paraxial marginal ray and the principal ray, and the calculation amount is small. The as-built performance evaluation model can be directly used as error function in optical design software for optical system optimization. A Cooke triplet system is taken as an example to compare the as-built performance optimization method, Code V and Zemax OpticStudio's built-in optimization methods and the traditional method which optimizes only nominal performance by Monte-Carlo tolerance analysis.

1. Introduction

In the production process of the optical system, the manufacture and alignment errors of the optical components can cause deterioration in imaging quality and make designer fail to achieve nominal performance. Therefore, the good as-built performance of an optical system should be the ultimate goal pursued by optical designers compared to the nominal performance. Loose tolerance requirements can reduce the difficulty of manufacture and alignment, improve yield and reduce production costs. At present, the traditional optical design process isolates the two processes of optical system optimization and tolerance allocation. The optical design optimization process does not consider the influence of image quality degradation caused by the manufacture and alignment errors, and only pursues the best nominal performance. The tolerance requirements need to be further analyzed after the design is completed. This often leads to good nominal performance, but the manufacture and alignment tolerances are tight. In this case, the design needs to be re-optimized, which is time-consuming. At the same time, there is no guarantee that the redesigned structure will have excellent as-built performance. Therefore, how to optimize the optical system as-built performance is an urgent problem to be solved.

In response to this problem, many researchers have done a series of studies, which can be divided into two categories: analytical methods and numerical methods. Numerical methods are more common in recent years.

Numerical methods generally rely on complex global optimization algorithms and a large number of ray tracing processes to obtain design results. The numerical methods are mainly as follows: global optimization method, ray incidence angle or deflection angle optimization method.

Rogers [1] builds multiple configurations based on the initial configuration to simulate the state of the optical system with quantitative manufacturing errors. He uses the global optimization function in Code V software to optimize this set of multiple configurations and tried to find an optimal design solution for as-built performance. McGuire [2] also uses the global optimization algorithm to obtain a large number of initial systems. Then he performs tolerance analysis on these systems, sorts their as-built performance and finds the best as-built performance system. Both methods are easy to operate, and the evaluation of the optical system as-built performance can be considered unbiased. However, to obtain unbiased and accurate optimization results, the number of multiple configurations to be built usually needs to be very large, or it is necessary to perform tolerance analysis and as-built performance evaluation on a very large number of systems, and also multiple fields of view need to be considered, which requires a large amount of calculation and optimization time. For example, John R. Rogers' method only established three multiple configurations to simulate the as-built state, and optimized a system with 11 lenses, which took 25 hours.

The ray incidence angle or deflection angle optimization method [3–5] uses incident angle or deflection angle of the typical ray (usually using the marginal ray) on the optical surface as an indicator for evaluating the sensitivity of the components. The method is easy to implement and has a certain desensitization design effect. However, this method is not accurate in evaluating as-built performance.

Liu et al. [6] proposed a design method for a low-sensitivity free-form reflective optical system. Based on the point-by-point design method, the method first designs a spherical reflection system and then performs sensitivity analysis to preferentially convert the low-sensitivity optical surfaces into an aspheric or free-form surface. The above steps are repeated a plurality of times. The configuration with the best as-built performance is selected from the plurality of free-form optical systems by performing sensitivity analysis. This method is suitable for the design of free-form systems, but its principle is similar to the global optimization method, which relies on a large number of ray tracing for image quality and sensitivity evaluation, and the calculation amount is large.

In addition, some commercial optical design software also has built-in numerical as-built performance optimization algorithms. For example, Code V's built-in Sensitivity As Built (SAB) method completes the as-built performance evaluation by calling the wavefront differential tolerancing algorithm. Zemax OpticStudio's built-in "TOLR" method evaluates as-built performance by calling the tolerance sensitivity analysis function.

The analytical design method refers to the optimization design of the optical system as-built performance by using the aberration theory as a design guide. It is represented by the design method proposed by Catalan [7], Meng et al. [8], Bauman and Schneider [9].

Catalan [7] deduced the approximation function expression between the decenters, the tilts and the axial misalignment and the coma aberration for two mirror telescopes. Based on this, the design method of the two mirror telescope with low misaligned sensitivity is proposed. Meng et al. [8] analyzed the optical path difference of the off-axis three mirror telescope and found that the off-axis quantity is an important factor affecting the sensitivity of the optical components, and proposed a design method suitable for reducing misalignment sensitivity of off-axis three mirror systems. The method achieves good results. However, the above methods are suitable for the specific type of optical systems. The derived conclusions cannot be directly applied to other systems. The versatility of the method is poor, and in the case of a large number of optical components, the derivation process becomes complicated.

Bauman and Schneider [9] established a linear relationship model of the optical surface decenter, compensator and wave aberrations. It does not need to trace a large amount of rays, which greatly reduces the system optimization time, and the method is highly versatile. However, to realize the matrix operation, the quadratic terms of the aberration field decenter vector in

the nodal aberration theory is ignored in the approximation process. At the same time, there is no analytical derivation of the influence of manufacture and alignment errors on wavefront aberration.

Aiming at the above problems, this paper establishes an optical system as-built performance evaluation model based on nodal aberration theory, and deduces the analytical expressions of optical component manufacture and alignment errors (decenter and tilt of optical surface) and aberration introduced by misalignments. The specific optical design parameters related to the optical component tolerance sensitivity are analyzed to provide theoretical guidance for optimal design of optical system as-built performance.

This paper mainly includes the following aspects: Section 2 introduce the establishment process of optical system as-built performance evaluation model. Section 3 deduce the analytical relationship between the optical surface decenters and tilts and the coma and astigmatism introduced by misalignments in detail. We optimize a Cooke triplet system using the as-built performance evaluation model, and compare the optimization results of the traditional method, Code V and Zemax OpticStudio's built-in optimization methods and the new method by Monte-Carlo tolerance analysis in section 4. We summarize the full paper in section 5. The appendix gives an analytical form of the aberration field decenter vector for all surfaces when a surface in the optical system misaligned.

2.   The establishment of optical system as-built performance evaluation model

In misaligned optical systems, the manufacture and alignment errors can be divided into axisymmetric and non-axisymmetric. Axisymmetric errors include lens spacing errors, lens thickness errors, and curvature radius errors. This type of error mainly introduces the spherical aberration, which is a field-constant aberration. The non-axisymmetric errors mainly refer to the decenters and tilts of the optical surface. Such errors mainly introduce the asymmetric coma and astigmatism in the field of view, which are the main aberrations that cause the optical system to degrade in image quality after the manufacturing process is completed. In the alignment, the spherical aberration introduced by manufacturing errors can be compensated by adjusting the axial position of a certain lens, which is easier to control than the coma and astigmatism, so it is not included in the study. In addition, the manufacture and alignment errors will also cause changes in field curvature and distortion. Distortion will not reduce the imaging clarity. The effect of the field curvature introduced by misalignments is generally small, so these two aberrations are also not studied in this paper. Therefore, the coma and astigmatism introduced by the decenters and tilts of the optical surface are the focus of this paper.

Wavefront aberrations are selected as the evaluation indicator of optical system as-built performance because it is suitable for performance evaluation of most imaging optical systems. Then the optical system as-built performance A can be evaluated by

$$A = \frac{\int_{field} \sqrt{|N(\boldsymbol{H})|^2 + |M(\boldsymbol{H})|^2} \, d\boldsymbol{H}}{\int_{field} d\boldsymbol{H}}, \tag{1}$$

where $|N(\boldsymbol{H})|$ represents the nominal value of Root Mean Square (RMS) wave aberration of the optical system in the field $\boldsymbol{H}$. $|M(\boldsymbol{H})|$ represents the RMS wave aberration introduced by the manufacture errors in the field $\boldsymbol{H}$. The average of the wave aberrations in the full field of view is taken to represent the optical system as-built performance. In this paper, the vector parameters are always expressed in black italics to facilitate the reader to distinguish between scalars and vectors, and the absolute value symbol indicates the modulo of the vectors.

The key to the establishment of the optical system as-built performance model is to obtain the analytical form of $|M(\boldsymbol{H})|$. The contribution to the wave aberration can be calculated separately

in the case where each manufacture error acts alone, and then the root-sum-of-squares (RSS) of all the wave aberration contributions is taken to obtain $|M(H)|$, as shown in Eq. (2):

$$|M(H)| = \sqrt{\sum_k [|M(H)_{k,\text{coma,T}}|^2 + |M(H)_{k,\text{coma,D}}|^2 + |M(H)_{k,\text{ast,T}}|^2 + |M(H)_{k,\text{ast,D}}|^2]}, \quad (2)$$

where k is the surface number, the subscript coma represents coma aberration, the subscript ast represents astigmatism aberration, the subscript T represents tilt error, and the subscript D represents decenter error. For example, $M(H)_{k,\text{coma,T}}$ represents the coma contribution of the tilt error of the k-th surface in the optical system in the field H. Its modulo represents the RMS value of the coma, and its direction represents the direction of the coma. The specific expressions of $M(H)_{k,\text{coma,T}}$, $M(H)_{k,\text{coma,D}}$, $M(H)_{k,\text{ast,T}}$, and $M(H)_{k,\text{ast,D}}$ will be derived below.

3. Misalignment-induced coma and astigmatism

The nodal aberration theory is to study the aberration theory of optical system with decentered and tilted components. Its original idea was proposed by Shack [10]. Buchroeder [11] and Thompson [12–14] do a lot of work on the theory later, which make the nodal aberration theory further developed. According to this theory, the aberration fields of the decentered and/or tilted optical surfaces in the system are all rotationally symmetric, and the total aberration field is still the sum of the aberration field contribution of each surface. This is the same as the rotationally symmetric optical systems. Only the center of the aberration field of the decentered and/or tilted optical surface is offset from the center of the field of view. This offset is represented by the vector σ, and its value is related to the decenters and tilts. The total aberration field of the system is obtained by adding the aberration fields of each surface in a misaligned manner. Therefore, the total aberration field of the system is usually not rotationally symmetric, and can be expressed by Eq. (3) [13]:

$$W(H, \rho) = \sum_j \sum_{p=0}^{\infty} \sum_{n=0}^{\infty} \sum_{m=0}^{\infty} W_{klm}^{(j)}[(H - \sigma^{(j)}) \cdot (H - \sigma^{(j)})]^p (\rho \cdot \rho)^n [(H - \sigma^{(j)}) \cdot \rho]^m, \quad (3)$$

where the superscript (j) is the surface number, $W_{klm}^{(j)}$ is the wave aberration coefficient for surface j, H denotes the field vector, and ρ is the pupil vector. Since the misalignments in the imaging optical system are usually small, the third-order aberrations accounts for the main contribution in the misalignment-induced aberrations, and the high-order aberrations can be ignored. Therefore, the three-order coma and astigmatism introduced by the misalignments are deduced below.

3.1. Misalignment-induced three-order coma

According to the nodal aberration theory, the third-order coma of decentered and/or tilted optical systems can be expressed by Eq. (4) [13]:

$$W_{COMA_3} = \sum_j W_{131}^{(j)}[(H - \sigma^{(j)}) \cdot \rho](\rho \cdot \rho). \quad (4)$$

Equation (4) can be modified to decompose the third-order coma of the decentered and/or tilted optical system into the system's intrinsic coma and the misalignment-induced coma, as expressed

by Eq. (5):

$$W_{COMA_3} = \underbrace{\left[\left(\sum_j W_{131}^{(j)} \boldsymbol{H}\right) \cdot \boldsymbol{\rho}\right](\boldsymbol{\rho} \cdot \boldsymbol{\rho})}_{\text{intrinsic coma}} \quad \underbrace{-\left[\sum_j W_{131}^{(j)} \boldsymbol{\sigma}^{(j)} \cdot \boldsymbol{\rho}\right](\boldsymbol{\rho} \cdot \boldsymbol{\rho})}_{\text{misalignment - induced field - constant coma}} . \tag{5}$$

Therefore, the misalignment-induced coma is the field constant coma, which is the sum of the misalignment-induced coma contributions of all surfaces in the optical system, and its RMS value and direction are expressed by Eq. (6):

$$\boldsymbol{M}(\boldsymbol{H})_{\text{coma}} = \sum_j \boldsymbol{M}(\boldsymbol{H})_{\text{coma}}^{(j)} = \sum_j \left(-\frac{1}{2\sqrt{2}} W_{131j} \boldsymbol{\sigma}^{(j)}\right), \tag{6}$$

where $\boldsymbol{M}_{\text{coma}}^{(j)}$ denotes misalignment-induced coma contribution of the j-th surface in the optical system.

The aberration field decenter vectors of the optical surfaces can be obtained by tracing the Optical Axis Ray (OAR, the ray that is emitted from the center of the field of view and passes through the center of the aperture stop) [14]. Therefore, in an optical system including n optical surfaces, in the case where the k-th surface is decentered and/or tilted, the aberration field decenter vectors of the optical surface j can be expressed by

$$\boldsymbol{\sigma}^{(j)}{}_k = \frac{(\boldsymbol{T}_k + c_k \boldsymbol{D}_k)}{\bar{i}_j} \alpha_j, \tag{7}$$

where

$$\alpha_j = \begin{cases} 0 & \text{while } j = 1, 2, \cdots, k-1 \\ 1 & \text{while } j = k \\ (i_j \cdot \bar{y}_k - \bar{i}_j \cdot y_k)\frac{\Delta n_k}{\mathcal{H}}, & \text{while } j = k+1, k+2, \cdots, n \end{cases}, \tag{8}$$

where $\boldsymbol{T}_k$ and $\boldsymbol{D}_k$ denote the tilt and decenter of the k-th surface, c_k denotes the curvature of the k-th surface. Since the decenter error can be equivalent to the tilt error for the spherical surface, $(\boldsymbol{T}_k + c_k \boldsymbol{D}_k)$ is called the equivalent tilt parameter. i_j and $\bar{i}_j$ denote the marginal ray incident angle and the principal ray incident angle on the j-th surface. y_k and $\bar{y}_k$ denote the heights of the marginal ray and the principal ray. $\Delta n_k = n_k' - n_k$, which denotes the change of refractive index across interface of the k-th surface. $\mathcal{H}$ denotes the optical invariant. See the appendix for the detailed derivation process.

According to the Seidel coma formula:

$$W_{131} = -\frac{1}{2} i \,\bar{i} y n^2 \Delta\left(\frac{u}{n}\right), \tag{9}$$

where $\Delta\left(\frac{u}{n}\right)$ denotes the so-called "aplanatic" parameter.

Substituting Eqs. (7)–(9) into Eq. (6), it can be obtained that when the k-th surface is misaligned in the optical system, the misalignment-induced coma is

$$\boldsymbol{M}(\boldsymbol{H})_{k,\text{coma}} = \sum_{j=1}^{n} \boldsymbol{M}(\boldsymbol{H})_{k,\text{coma}}^{(j)} = \underbrace{\left[\sum_{j=k}^{n} \frac{1}{4\sqrt{2}} i_j \, n_j{}^2 y_j \Delta\left(\frac{u}{n}\right)_j \alpha_j\right]}_{\substack{\text{sensitivity coefficient of the misalignment - induced} \\ \text{coma to the equivalent tilt parameter}}} (\boldsymbol{T}_k + c_k \boldsymbol{D}_k). \tag{10}$$

In Eq. (10), let $\boldsymbol{D}_k = \begin{bmatrix} 0 \\ 0 \end{bmatrix}$, then we can get the expression of the misalignment-induced coma when there is only tilt misalignment; let $\boldsymbol{T}_k = \begin{bmatrix} 0 \\ 0 \end{bmatrix}$, we can get the expression of the misalignment-induced coma when there is only decenter misalignment. The term in the square bracket is commonly known as the sensitivity coefficient of the misalignment-induced coma to the misalignments, which indicates the sensitivity of the misalignments.

So far, we derive the expression of the coma introduced by the decenters and tilts of the optical components. The total misalignment coma of the system is the sum of the misalignment coma introduced by each surface. It can be seen from Eq. (10) that the coma contribution of each surface is linear with the equivalent tilt parameter. According to the value of α_j, the optical surfaces can be divided into three categories: the surfaces before the decentered and/or tilted surface, the decentered and/or tilted surface itself and the surfaces behind the decentered and/or tilted surface. There is no misalignment aberration contribution on the optical surfaces before the decentered and/or tilted surface. For the decentered and/or tilted surface itself, its coma contribution is proportional to the incident angle of the marginal ray, the height of the marginal ray, the square of the local object space refractive index, and the "aplanatic" parameter of the surface. For the surfaces behind the decentered and/or tilted surface, the scale factor has one more parameter $(i_j \cdot \bar{y}_k - \bar{i}_j \cdot y_k)\Delta n_k / \mathcal{K}$, which differs from the decentered and/or tilted surface itself.

3.2. Misalignment-induced three-order astigmatism

The astigmatism of the misaligned optical system can be expressed by Eq. (11) [13]:

$$W_{ATS3} = \frac{1}{2} \sum_j W_{222}^{(j)} [(\boldsymbol{H} - \boldsymbol{\sigma}^{(j)})^2 \cdot \boldsymbol{\rho}^2]. \tag{11}$$

Similar to the processing of the coma, Eq. (11) is deformed to decompose the third-order astigmatism of the misaligned optical system into the system's intrinsic astigmatism and misalignment-induced astigmatism, as shown in Eq. (12):

$$W_{ATS3} = \underbrace{\sum_j \frac{1}{2} W_{222}^{(j)} \boldsymbol{H}^2 \cdot \boldsymbol{\rho}^2}_{\text{intrinsic astigmatism}} \underbrace{-(\sum_j W_{222}^{(j)} \boldsymbol{H} \boldsymbol{\sigma}^{(j)}) \cdot \boldsymbol{\rho}^2}_{\substack{\text{misalignment - induced} \\ \text{field - linear } \textit{astigmatism}}} + \underbrace{\sum_j \frac{1}{2} W_{222}^{(j)} \boldsymbol{\sigma}^{(j)2} \cdot \boldsymbol{\rho}^2}_{\substack{\text{misalignment - induced} \\ \text{field - constant } \textit{astigmatism}}}. \tag{12}$$

The misalignment-induced astigmatism is divided into two types, one is the field-linear astigmatism, and the other is the field-constant astigmatism. The RMS value and direction of the misalignment-induced astigmatism can be represented by

$$\boldsymbol{M}(\boldsymbol{H})_{\text{ast}} = \sum_j \boldsymbol{M}(\boldsymbol{H})_{\text{ast}}^{(j)} = \sum_j -\frac{1}{\sqrt{6}} W_{222}^{(j)} \boldsymbol{H} \boldsymbol{\sigma}^{(j)} + \sum_j \frac{1}{2\sqrt{6}} W_{222}^{(j)} \boldsymbol{\sigma}^{(j)2}, \tag{13}$$

where $\boldsymbol{M}(\boldsymbol{H})_{\text{ast}}^{(j)}$ denotes misalignment-induced astigmatism contribution of the j-th surface in the optical system.

According to the Seidel astigmatism formula:

$$W_{222} = -\frac{1}{2}\bar{i}^2 y n^2 \Delta\left(\frac{u}{n}\right). \tag{14}$$

Substituting Eqs. (7), (8) and (14) into Eq. (13). it can be obtained that when the *k*-th surface is misaligned in the optical system, the misalignment-induced astigmatism is

$$
\begin{aligned}
M(H)_{k,\text{ast}} &= \sum_{j=1}^{n} M(H)_{k,\text{ast}}^{(j)} = \sum_{j=k}^{n}\left[\frac{1}{2\sqrt{6}}\bar{i}_j\, y_j\, n_j^{\,2}\Delta\left(\frac{u}{n}\right)_j H\alpha_j\right](T_k + c_k D_k)\\
&\quad - \sum_{j=k}^{n}\left[\frac{1}{4\sqrt{6}}y_j\, n_j^{\,2}\Delta\left(\frac{u}{n}\right)_j\alpha_j^{\,2}\right](T_k + c_k D_k)^2.
\end{aligned}
\tag{15}
$$

In Eq. (15), let $D_k = \begin{bmatrix} 0 \\ 0 \end{bmatrix}$, then we can get the expression of the misalignment-induced astigmatism when there is only tilt misalignment; let $T_k = \begin{bmatrix} 0 \\ 0 \end{bmatrix}$, we can get the expression of the misalignment-induced astigmatism when there is only decenter misalignment.

Similar to the case of coma, when an optical surface is misaligned, the surface in front of the misaligned surface will not introduce misalignment aberration. Only the misaligned surface itself and a series of surfaces behind the misaligned surface will do. The misalignment-introduced astigmatism is divided into two parts: field-linear astigmatism and field-constant astigmatism. The field-linear astigmatism is proportional to the equivalent tilt parameter. For the decentered and/or tilted surface itself, the proportional coefficient is related to the principal ray incident angle, the height of the marginal ray, the square of the local object space refractive index and the "aplanatic" parameter. For the optical surfaces after the decentered and/or tilted surface, the proportionality factor is increased by a factor $(i_j \cdot \bar{y}_k - \bar{i}_j \cdot y_k)\Delta n_k/\mathcal{H}$. The field-constant astigmatism is proportional to the square of the equivalent tilt parameter. For the decentered and/or tilted surface itself, the proportional coefficient is related to the height of the marginal ray, the square of the local object space refractive index and the "aplanatic" parameter. For the optical surfaces after the decentered and/or tilted surface, the proportionality factor is increased by a factor $(i_j \cdot \bar{y}_k - \bar{i}_j \cdot y_k)^2\Delta n_k^{\,2}/\mathcal{H}^2$.

It can be seen that the total misalignment-introduced astigmatism and the decenters/tilts are quadratic relations. The field-constant astigmatism can be considered as terms of higher order than the field-linear astigmatism. Therefore, when the misalignments are very small, the quadratic term (the field-constant astigmatism) can be ignored. The misalignment aberration is dominated by field-linear astigmatism. The misalignment-introduced astigmatism can be approximated as a linear function of the equivalent tilt parameter, as shown in Eq. (16):

$$
M(H)_{k,\text{ast}} = \underbrace{\left[\sum_{j=k}^{n}\frac{1}{2\sqrt{6}}\bar{i}_j\, y_j\, n_{1j}^{\,2}\Delta\left(\frac{u}{n}\right)_j H\alpha_j\right]}_{\substack{\text{sensitivity coefficient of the misalignment - induced} \\ \text{astigmatism to the equivalent tilt parameter}}} (T_k + c_k D_k).
\tag{16}
$$

The term in the square bracket is the sensitivity coefficient of the misalignment astigmatism to the equivalent tilt parameter at the field H.

In this paper, we still retain the contribution of the field-constant astigmatism during the establishment process of the as-built performance evaluation model to improve the accuracy of

the model. After substituting Eqs. (10) and (15) into Eq. (2), we can obtain the optical system as-built performance evaluation model.

In addition to the quantitative calculation of as-built performance, the analysis results in this section can also help optical designers to qualitatively determine whether the tolerances of optical surfaces are tight. According to the analysis results, the incident angle and the height of the marginal ray and the incident angle of the principal ray on the surface are closely related to the tolerance requirements. The larger the three parameters, the tighter the tolerances of the optical surface. Optical designers often call the lens which is quite well behaved with no steep bending or severe angles of incidence as "happy lens". The advantage of this lens is that the tolerances is loose. This is the experience that optical designers have summarized over the years. This experience is in good agreement with the results of this paper. It can also be seen that the influence of the decenters and tilts of the rear surface of the lens is generally greater than that of the front surface, since the misalignment aberration is also related to the local object space refractive index. Due to the third-order coma and astigmatism coefficient are proportional to the "aplanatic" parameter, so it can be considered to some extent that a relatively large misalignment aberration is introduced when the optical surface with large third-order aberration coefficients is decentered and/or tilted.

4. Optimization example

4.1. Initial optical system

In this section, we will optimize a Cooke triplet system. Firstly, we use the traditional method to optimize the nominal performance of the system with software Code V 11.1, and then the as-built performance optimization method proposed in this paper is used. In addition to comparing as-built performance, we also use Code V's built-in (SAB) method and Zemax OpticStudio's built-in "TOLR" method to optimize the as-built performance. Finally, we will use Monte Carlo tolerance analysis to evaluate and compare the as-built performance of the optimization results of the four methods. We set the decenter and tilt of all surfaces as system manufacturing tolerances, and the tolerance distribution is uniformly distributed. In tolerance analysis, the maximum value of the tolerance on decenters in x and y directions of each surface is set to 0.1 mm, and the maximum value of the tolerance on tilts about x and y axes is set to 23'. The tilt angle and the position of the image plane are used as compensators

The Cooke triplet system is taken from the sample lens library in Code V. The lens design parameters are shown in Table 1.

Table 1. lens data of Cooke triplet system

Surface	Surface type	Radius (mm)	Thickness (mm)	Glass	Semi-aperture (mm)
Object	sphere	infinity	infinity		
1	sphere	16.878	3.250	NSK16	8.11
2	sphere	247.026	4.984		7.55
3(stop)	sphere	−35.957	1.250	NF2	3.85
4	sphere	15.886	6.099		4.28
5	sphere	49.081	3.250	NSK16	8.36
6	sphere	−27.621	38.714		8.66
7(image)	sphere	infinity	-		17.94

The original lens has an entrance pupil diameter of 10 mm, a focal length of 50 mm, and a half field of view of 20°. The wavelength data are 546.1 nm (weight: 2), 486.1 nm (weight: 1) and 656.3 nm (weight: 1), respectively. Since the actual imaging usually uses a square field of view, the field of view is changed to 14°×14° in the optimization, and the vignetting is removed. The

aberration field of the optical system will no longer be symmetrical due to the misalignments of the optical elements, so 25 field points distributed at equal intervals in the 14°×14° field of view are selected for optimization to more accurately evaluate system performance, as shown in Fig. 1.
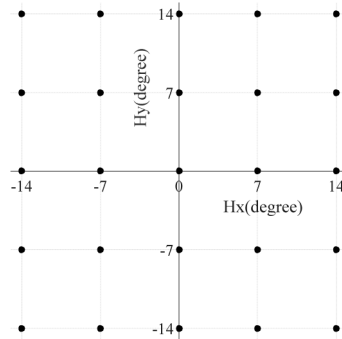
Fig. 1. Field points selected for optical system optimization, which is marked with black dots.

4.2. Case 1: Traditional optimization method

First, we use traditional optimization method to optimize only the nominal performance. All the radius of curvature and thickness are set as the optimization variables. The system focal length limit is added in the specific constraints menu to make the focal length equal to 50 mm, so that the focal length remains unchanged during the optimization process. The wavefront error variance is set to error function for optimization. The standard optimization method in Code V is used. The optimized optical system is shown in Table 2.

Table 2. Lens data obtained by traditional optimization method

Surface	Surface type	Radius (mm)	Thickness (mm)	Glass	Semi-aperture (mm)
Object	sphere	infinity	infinity		
1	sphere	13.296	2.527	NSK16	6.27
2	sphere	337.649	3.118		5.89
3(stop)	sphere	−41.917	1.000	NF2	3.95
4	sphere	12.606	6.391		4.01
5	sphere	46.199	2.262	NSK16	6.97
6	sphere	−35.535	38.982		7.18
7(image)	sphere	infinity	-		17.39

4.3. Case 2: Our as-built performance optimization method

Then, we use the as-built performance evaluation model in this paper to establish the error function in the form of user-defined Macro-PLUS function, while the focal length limit is still added to the specific constraints. The selection of the optimization variables remains the same, then the initial system in Table 1 is optimized.

In the as-built performance evaluation model, the decenter value D_k and the tilt value T_k are set to the 0.0399 mm and 9.176', which are the mean of two-dimensional decenter and tilt tolerance, and are also equal to 0.399 times the maximum value of two-dimensional decenter and tilt tolerance. The wavelength of 546.1 nm is selected for calculation

The optical system optimized by the local optimization algorithm is shown in the Table 3. The evaluation of as-built performance only needs to trace the paraxial principal and marginal rays, so the calculation amount is small, and the optimization process can be completed in 1-2 minutes. The CPU used in the optimization is Intel Core. i7-7700HQ @ 2.80 GHz.

Table 3. Lens data obtained by our as-built performance optimization method

Surface	Surface type	Radius (mm)	Thickness (mm)	Glass	Semi-aperture (mm)
Object	sphere	infinity	infinity		
1	sphere	16.949	3.297	NSK16	7.26
2	sphere	281.318	5.000		6.61
3(stop)	sphere	−34.716	1.198	NF2	3.66
4	sphere	16.097	5.881		3.91
5	sphere	48.859	2.741	NSK16	7.03
6	sphere	−27.714	38.460		7.33
7(image)	sphere	infinity	-		17.42

4.4. Case 3: Code V's built-in SAB method

Code V's built-in SAB method can be used in automatic design for improving the as-built performance by using wavefront differential coefficients to reduce the tolerance sensitivity. We used the SAB method to optimize the initial system to compare the optimization results. The optimization variables and tolerance values are set the same as in case 2, and the image plane position and tilt are set as compensators. The optimization takes about 1-2 minutes. The system obtained by the optimization are shown in Table 4.

Table 4. Lens data obtained by the SAB method

Surface	Surface type	Radius (mm)	Thickness (mm)	Glass	Semi-aperture (mm)
Object	sphere	infinity	infinity		
1	sphere	16.435	4.423	NSK16	6.98
2	sphere	493.583	3.777		5.93
3(stop)	sphere	−36.204	0.950	NF2	3.71
4	sphere	15.672	6.217		3.91
5	sphere	51.659	2.354	NSK16	7.06
6	sphere	−29.266	38.435		7.28
7(image)	sphere	infinity	-		17.39

4.5. Case 4: Zemax OpticStudio's built-in TOLR method

The Zemax OpticStudio software also includes tolerance sensitivity optimization method. The optimization operand "TOLR" can be used to optimize for reduced sensitivity to tolerances. The optimization settings remain the same. After about 8 hours of optimization, the system shown in Table 5 can be obtained.
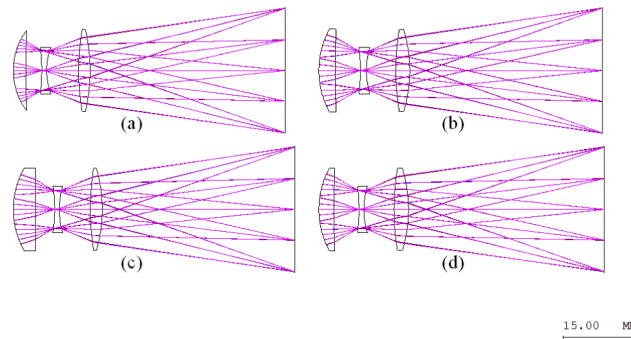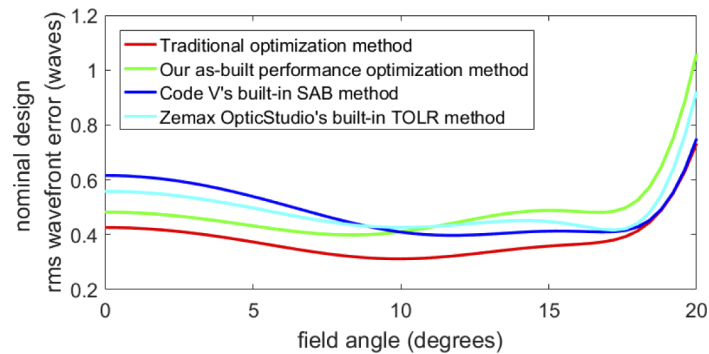
## 4.6. Comparison of optimization results

The optical systems optimized by the above 4 methods are shown in Fig. 2.

The nominal performance (rms wavefront error vs. field angle) of the optical system obtained by the four optimization methods are shown in Fig. 3.

Table 5. Lens data obtained by the TOLR method

Surface	Surface type	Radius (mm)	Thickness (mm)	Glass	Semi-aperture (mm)
Object	sphere	infinity	infinity		
1	sphere	16.876	3.051	NSK16	7.83
2	sphere	248.649	4.950		7.32
3(stop)	sphere	−35.668	1.017	NF2	3.80
4	sphere	16.040	6.016		4.16
5	sphere	49.607	2.828	NSK16	7.92
6	sphere	−27.622	39.121		8.17
7(image)	sphere	infinity	-		17.37

Fig. 2. Optical systems optimized by (a) the traditional optimization method, (b) our as-built performance optimization method, (c) the SAB method and (d) the TOLR method.

Fig. 3. The nominal performance (rms wavefront error vs. field angle) of optical systems obtained by the traditional optimization method, our as-built performance optimization method, the SAB method and the TOLR method.
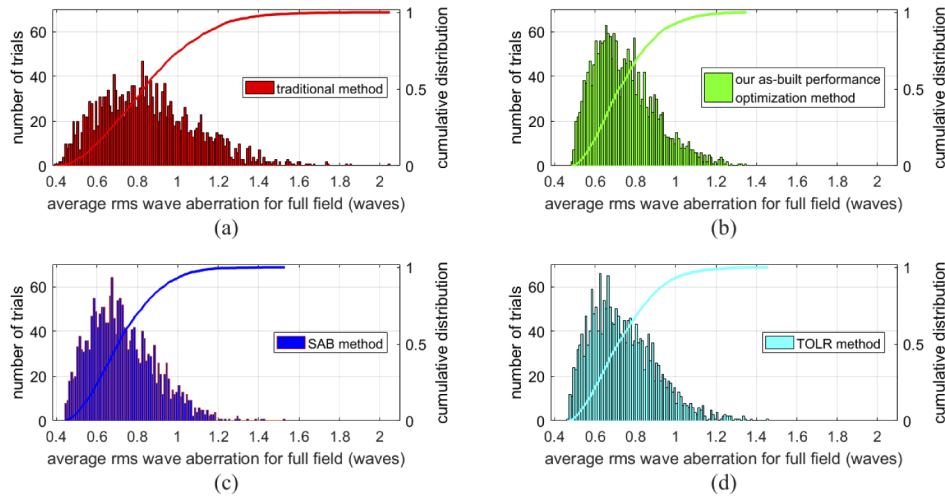
Fig. 4. Monte-Carlo tolerance analysis results of the optical system obtained by (a) the traditional optimization method, (b) our as-built performance optimization method, (c) the SAB method and (d) the TOLR method. The full-field average wave aberration rms values distribution histogram and cumulative curve for 2000 tolerance samples are shown.

It can be seen from Fig. 3 that the nominal value of the wavefront aberration of the optical system optimized by the traditional method is lower than those of the other three optimization methods. The full-field average wave aberration rms value obtained by the traditional method is 0.383 waves, while those obtained by our method, the SAB method and the TOLR method are 0.484 waves, 0.486 waves and 0.489 waves, respectively.

Now we will compare the as-built performance of these four systems. We used the Monte-Carlo tolerance analysis method with 2000 samples to predict the as-built performance. The full-field average wave aberration rms values of 2000 Monte-Carlo samples are statistically analyzed. The statistical results are shown in Fig. 4 and Table 6.

Table 6. Comparison of four optimization methods

Average rms wave aberration for full field	Traditional method	Our method	SAB method	TOLR method
Algorithm type	-	Analytical	Numerical	Numerical
Number of rays to be traced for as-built performance evaluation	-	Only need to trace two paraxial rays	32 rays traced across the pupil diameter for each field	4 rings, and 8 arms selected
Time required	Less than 5s	1-2 min	1-2 min	8 hours
Nominal value (waves)	0.349	0.454	0.440	0.453
80th percentile (waves)	1.055	0.872	0.863	0.871
Maximum value (waves)	2.048	1.349	1.529	1.456
Standard deviation (waves)	0.243	0.155	0.165	0.163

As can be seen from Table 6, the nominal value of wavefront aberration of the optical system designed by the traditional method is smaller than those of the systems obtained by the other three method by about 0.1 waves. However, according to the Monte-Carlo tolerance analysis results, the as-built performance of the optical system optimized by the traditional method shows serious degradation. For the 80th percentile of rms wave aberration, the result obtained by our

method is 0.183 waves smaller than the traditional method. The results obtained by the three as-built optimization methods are not much different, and the SAB method optimization results are slightly better. The maximum wave aberration of the samples obtained by our method is 0.699 waves, 0.180 waves, and 0.107 waves smaller than those of the traditional method, the SAB method, and the TOLR method, respectively. At the same time, the standard deviation of the wave aberration of all samples obtained by our as-built performance optimization method is only 64% of that of the traditional method, which indicates that the optical system obtained by our method is less sensitive to tolerances.

Both the SAB method and the TOLR method are numerical algorithms, which need to trace a large number of rays to complete the evaluation of system as-built performance. Our method only needs to trace two paraxial rays to complete the calculation. From the perspective of optimization time, both our method and SAB method can complete the optimization in 1 to 2 minutes, while the TOLR method takes 8 hours.

5. Conclusions

We propose an analytical method for optical system as-built performance optimization based on nodal aberration theory. This method can evaluate the optical system as-built performance by only tracking the paraxial principal ray and marginal ray. We derive the analytical relationship between the surface decenters and tilts that are two most common manufacturing tolerances and the as-built performance in the form of wave aberrations. The influence of optical surface decenter and tilt tolerances on as-built performance is related to the incident angles of the principal ray and the marginal ray, the heights of the principal ray and the marginal ray, the local object space refractive index, the "aplanatic" parameter and the invariant. The as-built performance evaluation model can be edited and saved in the form of a macro file in the optical design software, which can be used as a user-defined error function to optimize the optical system. The Cooke triplet system optimization example and Monte-Carlo tolerance analysis show that although the nominal value of system wave aberration of the as-built performance optimization method is 0.105 waves larger than that of the traditional method, the 80th percentile of Monte-Carlo tolerance sample's wave aberration is 0.183 waves smaller than that of the traditional method. In addition, we also compared our method with Code V's built-in SAB method and Zemax's built-in TOLR method. The optimization results of these three methods are similar. The optimization efficiency of our method is similar to the SAB method, which is much better than the TOLR method.

Appendix: Derivation for aberration field decenter vectors for optical system in which a surface is decentered and/or tilted

The OAR tracing method used in the derivation for the aberration field decenter vectors was first proposed by Buchroeder [11].

a. Derivation of the centers of object/images and entrance/exit pupils in an optical system with tilted and/or decentered components

For any tilted and/or decentered optical surface, the centers of object/images (**Q**/ **Q'**) and the center of the entrance/exit Pupils (**E**/ **E'**) can be recursively calculated by Eqs. (17) and (18) in the order of the optical surfaces [14]:

$$\frac{\delta Q^{\#'}}{\bar{y}_o'} = \frac{\delta Q^{\#}}{\bar{y}_o} + (\frac{y\Delta n}{\mathcal{H}})(T + Dc), \tag{17}$$

$$\frac{\delta E^{\#'}}{y_E'} = \frac{\delta E^{\#}}{y_E} - (\frac{\bar{y}\Delta n}{\mathcal{H}})(T + Dc), \tag{18}$$

where $\delta Q^{\#}/\bar{y}_o$ and $\delta Q^{\#'}/\bar{y}_o'$ locate the center of the object field and center of the image field normalized by the paraxial field height, $\bar{y}_o$ and $\bar{y}_o'$. $\delta E^{\#}/y_E$ and $\delta E^{\#'}/y_E'$ locate the center of the entrance pupil and center of the exit pupil normalized by the pupil radius, y_E and y_E'.

b. Calculation of OAR parameters

The OAR can be described by two parameters: The slope angle of the OAR before refraction that is denoted as $\bar{u}_{OAR}^{\#}$ and the height from the mechanical reference axis of the OAR that is denoted as $\bar{y}_{OAR}^{\#}$. The mechanical reference axis is the optical axis in a rotationally symmetric optical system, which is unaffected by decenters and tilts. $\bar{u}_{OAR}^{\#}$ and $\bar{y}_{OAR}^{\#}$ can be calculated by

$$\bar{u}_{OAR}^{\#} = \bar{u}\frac{\delta Q^{\#}}{\bar{y}_o} + u\frac{\delta E^{\#}}{y_E}, \tag{19}$$

$$\bar{y}_{OAR}^{\#} = \bar{y}\frac{\delta Q^{\#}}{\bar{y}_o} + y\frac{\delta E^{\#}}{y_E}, \tag{20}$$

where u and $\bar{u}$ denote the slope angle of the marginal ray and principal ray.

c. Derivation of aberration field decenter vectors

The aberration field decenter vectors can be calculated using Eq. (21) [14]:

$$\sigma^{(j)} = -\frac{\bar{u}_{OAR,j}^{\#} + \bar{y}_{OAR,j}^{\#}c_j - (T_j + c_j D_j)}{\bar{i}_j}. \tag{21}$$

In an optical system that contains n optical surfaces, only the k-th optical surface is tilted and/or decentered, the surfaces before the k-th optical surface remains ideal, so

$$\bar{u}_{OAR,j}^{\#} = \begin{bmatrix} 0 \\ 0 \end{bmatrix}, \text{ while } j = 1, 2, \cdots, k. \tag{22}$$

$$\bar{y}_{OAR,j}^{\#} = \begin{bmatrix} 0 \\ 0 \end{bmatrix}, \text{ while } j = 1, 2, \cdots, k. \tag{23}$$

$$T_j = \begin{bmatrix} 0 \\ 0 \end{bmatrix}, \text{ while } j = 1, 2, \cdots, k-1. \tag{24}$$

$$D_j = \begin{bmatrix} 0 \\ 0 \end{bmatrix}, \text{ while } j = 1, 2, \cdots, k-1. \tag{25}$$

$$\sigma_k^{(j)} = \begin{bmatrix} 0 \\ 0 \end{bmatrix}, \text{ while } j = 1, 2, \cdots, k-1. \tag{26}$$

For the tilted and/or decentered surface k,

$$\sigma_k^{(k)} = \frac{(T_k + c_k D_k)}{\bar{i}_k}. \tag{27}$$

The optical surfaces after the tilted and/or decentered surface k is also maintained in an ideal state, so for these surfaces,

$$T_j = \begin{bmatrix} 0 \\ 0 \end{bmatrix}, \text{ while } j = k+1, k+2, \cdots, n, \tag{28}$$

$$\boldsymbol{D}_j = \begin{bmatrix} 0 \\ 0 \end{bmatrix}, \text{ while } j = k+1, k+2, \cdots, n. \tag{29}$$

However, because the k-th optical surface is tilted and/or decentered, the OAR no longer travels along the mechanical reference axis, so

$$\frac{\delta Q^{\#\prime}_j}{\bar{y}'_{o,j}} = \frac{\delta Q^{\#}_j}{\bar{y}_{o,j}} = \frac{\delta Q^{\#\prime}_k}{\bar{y}'_{o,k}} = (\frac{y_k \Delta n_k}{\mathcal{K}})(\boldsymbol{T}_k + \boldsymbol{D}_k c_k), \text{ while } j = k+1, k+2, \cdots, n, \tag{30}$$

$$\frac{\delta E^{\#\prime}_j}{y_{E,j}} = \frac{\delta E^{\#}_j}{y_{E,j}} = \frac{\delta E^{\#\prime}_k}{y'_{E,k}} = -(\frac{\bar{y}_k \Delta n_k}{\mathcal{K}})(\boldsymbol{T}_k + \boldsymbol{D}_k c_k), \text{ while } j = k+1, k+2, \cdots, n, \tag{31}$$

$$\bar{\boldsymbol{u}}^{\#}_{OAR,j} = (\bar{u}_j y_k - u_j \bar{y}_k)\frac{\Delta n_k}{\mathcal{K}}(\boldsymbol{T}_k + \boldsymbol{D}_k c_k), \text{ while } j = k+1, k+2, \cdots, n, \tag{32}$$

$$\bar{\boldsymbol{y}}^{\#}_{OAR,j} = (\bar{y}_j y_k - y_j \bar{y}_k)(\frac{\Delta n_k}{\mathcal{K}})(\boldsymbol{T}_k + \boldsymbol{D}_k c_k), \text{ while } j = k+1, k+2, \cdots, n. \tag{33}$$

Substituting Eqs. (32) and (33) into Eq. (21), we can get

$$\boldsymbol{\sigma}^{(j)}_k = \left[\frac{(u_j + y_j \cdot c_j) \cdot \bar{y}_k - (\bar{u}_j + \bar{y}_j c_j) y_k}{\bar{i}_j} \right] \frac{\Delta n_k}{\mathcal{K}}(\boldsymbol{T}_k + \boldsymbol{D}_k c_k) = \frac{(\boldsymbol{T}_k + c_k \boldsymbol{D}_k)}{\bar{i}_j}(i_j \cdot \bar{y}_k - \bar{i}_j \cdot y_k)\frac{\Delta n_k}{\mathcal{K}},$$
$$\text{while } j = k+1, k+2, \cdots, n. \tag{34}$$

Funding

Disclosures

The authors declare no conflicts of interest.

References

1. J. R. Rogers, "Using global synthesis to find tolerance-insensitive design forms," Proc. SPIE **6342**, 63420M (2006).
2. J. P. McGuire, "Designing easily manufactured lenses using a global method," Proc. SPIE **6342**, 63420O (2006).
3. M. Jeffs, "Reduced manufacturing sensitivity in multi-element lens systems," Proc. SPIE **4832**, 104–113 (2002).
4. M. Isshiki, L. Gardner, and G. G. Gregory, "Automated control of manufacturing sensitivity during optimization," Proc. SPIE **5249**, 343–352 (2004).
5. M. Isshiki, D. C. Sinclair, and S. Kaneko, "Lens design: global optimization of both performance and tolerance sensitivity," Proc. SPIE **6342**, 63420N (2007).
6. X. Liu, T. Gong, G. Jin, and J. Zhu, "Design method for assembly-insensitive freeform reflective optical systems," Opt. Express **26**(21), 27798–27811 (2018).
7. G. Catalan, "Design method of an astronomical telescope with reduced sensitivity to misalignment," Appl. Opt. **33**(10), 1907–1915 (1994).
8. Q. Meng, H. Wang, W. Wang, and Z. Yan, "Desensitization design method of unobscured three-mirror anastigmatic optical systems with an adjustment-optimization-evaluation process," Appl. Opt. **57**(6), 1472–1481 (2018).
9. B. J. Bauman and M. D. Schneider, "Design of optical systems that maximize asbuilt performance using tolerance/compensator-informed optimization," Opt. Express **26**(11), 13819–13840 (2018).
10. R. V. Shack and K. Thompson, "Influence Of Alignment Errors Of A Telescope System On Its Aberration Field," Proc. SPIE **0251**, 146–153 (1980).
11. R. A. Buchroeder, "Tilted Component Optical Systems," Ph.D. dissertation, (University of Arizona, 1976).
12. K. P. Thompson, "Aberration fields in tilted and decentered optical systems," Ph.D. dissertation, (University of Arizona, 1980).
13. K. Thompson, "Description of the third-order optical aberrations of near-circular pupil optical systems without symmetry," J. Opt. Soc. Am. A **22**(7), 1389–1401 (2005).
14. K. P. Thompson, T. Schmid, O. Cakmakci, and J. P. Rolland, "Real-ray-based method for locating individual surface aberration field centers in imaging optical systems without rotational symmetry," J. Opt. Soc. Am. A **26**(6), 1503–1517 (2009).